[Article] doi: 10.3866/PKU.WHXB201801263 www.whxb.pku.edu.cn

Catalytic Electroreduction of CO_2 to C_2H_4 Using Cu_2O Supported on 1-Octyl-3-methylimidazole Functionalized Graphite Sheets

NING Hui [1,2], WANG Wenhang [1], MAO Qinhu [1], ZHENG Shirui [1], YANG Zhongxue [1], ZHAO Qingshan [1], WU Mingbo [1,*]

[1] State Key Laboratory of Heavy Oil Processing, College of Chemical Engineering, China University of Petroleum, Qingdao 266580, Shandong Province, P. R. China.

[2] CAS Key Laboratory of Carbon Materials, Institute of Coal Chemistry, Chinese Academy of Sciences, Taiyuan 030001, P. R. China.

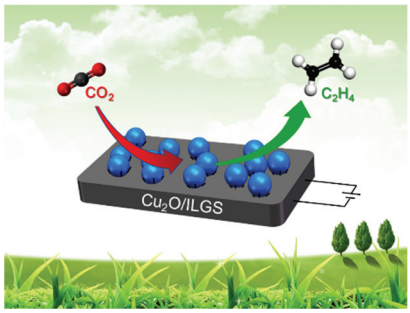

Abstract: The electrocatalytic reduction of CO_2 to C_2H_4 is a topic of great interest. It is known that the preparation of efficient catalysts for this transformation is the key factor that determines the yield of C_2H_4. In this study, we prepared 1-octyl-3-methylimidazole functionalized graphite sheets (ILGS) in a facile manner by the electro-exfoliation of pure graphite rod in an aqueous solution of 1-octyl-3-methylimidazolium chloride (OmimCl : H_2O = 1 : 5, *V*/*V*) at 10 V. They were then dispersed in an aqueous solution of copper chloride and sodium citrate. Subsequent reduction with sodium borohydride led to the formation of a composite comprised of cuprous oxide supported on Omim-functionalized graphite sheets (Cu_2O/ILGS). This composite was found to be an efficient catalyst for the electroreduction of carbon dioxide to ethylene. The as-made materials were characterized by transmission electron microscopy (TEM), X-ray photoelectron spectroscopy (XPS), Raman spectroscopy, and X-ray diffraction (XRD). The TEM images showed that the ILGS were composed of multiple layers of graphene. The XRD pattern and Raman spectrum indicated that the surface of the ILGS possessed several defects. In the electro-exfoliation process, the defects in the ILGS were modified in situ by covalent bonding with Omim groups, which was also confirmed by XPS. The Cu_2O nanoparticles with an average diameter of 5 nm were uniformly distributed on the surface of the ILGS because the Omim groups grafted to the graphite sheets acted as anchors and prevented their aggregation by the steric effect. The electrocatalytic activities of Cu_2O/ILGS for CO_2 reduction were measured at different voltages in 0.1 mol L^{-1} $KHCO_3$ aqueous solution under ambient temperature and pressure. These experiments showed that the catalytic performance of the Cu_2O/ILGS composite was determined by cuprous oxide, while the ILGS displayed nearly no catalytic activity in the electroreduction of carbon dioxide. The faradaic efficiency of hydrogen and carbon dioxide reduction products changed with the reaction time because of the reduction of Cu_2O to Cu under the electroreduction conditions. The faradaic efficiency of ethylene was ~14.8% at –1.3 V (*versus* reversible hydrogen electrode). The performance of Cu_2O/ILGS in the catalytic electroreduction of carbon dioxide was attributed to the stabilization of the Cu_2O nanoparticles by the nest-like microstructures in the Cu_2O/ILGS composite.

Key Words: Cu_2O; Graphite sheets; CO_2 reduction; Ethylene; Ionic liquids

Received: January 3, 2018; Revised: January 23, 2018; Accepted: January 23, 2018; Published online: January 26, 2018.

*Corresponding author. Email: wumb@upc.edu.cn; Tel.: +86-532-86983452.

The project was supported by the CAS Key Laboratory of Carbon Materials, China (KLCMKFJJ1706) and the National Natural Science Foundation of China (51372277, 51572296, U1662113).

中科院炭材料重点实验室开放基金(KLCMKFJJ1706)和国家自然科学基金(51372277, 51572296, U1662113)资助项目

1-辛基-3-甲基咪唑功能化石墨片负载氧化亚铜催化二氧化碳电还原制乙烯

宁汇[1,2]，王文行[1]，毛勤虎[1]，郑诗瑞[1]，杨中学[1]，赵青山[1]，吴明铂[1,*]

[1] 中国石油大学(华东)化学工程学院，重质油国家重点实验室，山东 青岛 266580

[2] 中国科学院炭材料重点实验室(中国科学院山西煤炭化学研究所)，太原 030001

摘要：电催化还原二氧化碳制备乙烯是备受关注的热点问题，高效催化剂的制备是决定乙烯产率的关键因素。本文在1-辛基-3-甲基咪唑氯的水溶液(OmimCl：H_2O = 1：5，体积比)中通过电剥离石墨棒制备了1-辛基-3-甲基咪唑功能化石墨片(ILGS)，在水溶液中负载氧化亚铜后得到氧化亚铜/1-辛基-3-甲基咪唑功能化石墨片复合材料(Cu_2O/ILGS)，通过透射电镜、X射线光电子能谱、拉曼光谱和X射线衍射对其组成和结构进行了系统研究，发现ILGS由多层石墨烯组成，表面富含缺陷。这些缺陷被1-辛基-3-甲基咪唑通过共价键修饰，形成类似鸟巢状的微结构，平均直径5 nm的Cu_2O纳米颗粒在石墨片表面均匀分散。在0.1 mol·L^{-1}碳酸氢钾水溶液中，研究了Cu_2O/ILGS在不同电压下催化CO_2电还原的性能。结果表明，Cu_2O是主要活性中心并在CO_2还原过程中被逐渐还原成铜，导致产物的法拉第效率随着反应时间而变，在−1.3 V (*vs* RHE)电压下，乙烯的法拉第效率最高达到14.8%，其性能归因于Cu_2O/ILGS复合材料中的鸟巢状微结构对Cu_2O纳米颗粒的稳定作用。

关键词：氧化亚铜；石墨片；二氧化碳还原；乙烯；离子液体

中图分类号：O646

1 Introduction

The electrochemical reduction of CO_2 to value-added chemicals is one of the best ways to recycle the CO_2 as C1 compounds resource and store electrical energy in chemical bonds [1–3]. Ethylene is a widely used chemical raw material in the world. The electrochemical reduction of CO_2 to ethylene under atmospheric conditions is a clean and promising route to replace the traditional ethylene production methods. Several new materials have been identified as electrocatalysts for the CO_2 reduction, with copper exhibiting the highest energetic efficiency and selectivity toward the formation of hydrocarbons, especially for producing ethylene.

In the recent years, numbers of strategies have been studied to increase the performance of Cu catalysts, including crystal surface [4,5] and morphology control [6–8], alloying [9], surface modification [10], composite construction [11] and oxidation treatment [12]. Among them, Cu_2O has gotten much attention due to its unique catalytic properties in CO_2 electroreduction. Above all, Cu_2O is considered as a promising precursor of cube metallic copper [13]. When used directly as a catalyst, the Cu_2O is firstly reduction to metallic Cu during the electrolysis while the CO_2 is reduced to C_2H_4 selectively on the Cu(100) surface [14]. The morphology of Cu can be controlled by the morphology of Cu_2O. Yeo *et al.* [15] prepared Cu_2O films of different thicknesses by galvanostatic deposition method on Cu disks and investigated the electrochemical reduction of CO_2 on Cu_2O films in aqueous 0.1 mol·L^{-1} $KHCO_3$ electrolytes. Through *ex situ* scanning electron microscopy, X-ray diffraction and *in situ* Raman spectroscopy, it is revealed that Cu_2O reduced rapidly and remained as metallic Cu^0 particles during the CO_2 reduction. In addition, they found the thin Cu films derived from Cu_2O have better selectivity than the thick ones, which indicates the thickness of Cu_2O precursor is closely related to the morphology of Cu [12]. In fact, it cannot be so sure that all the Cu_2O are reduced to Cu^0 during the electrolysis, some reports argue that there is remain some Cu(I) species on the surface of Cu. These Cu(I) species promote the selectivity of C_2H_4 and the bi-phase of Cu_2O-Cu is considered to be the active site for CO_2 electroreduction to ethylene [16]. The oxygen-vacant structures derived from the decrease in the oxygen concentration of the Cu_2O electrode during electrolysis has been confirmed by using bulk and surface-sensitive analytical techniques and the *in situ* formed structures play a critical role in maintaining the high reactivity of the electrode for C_2H_4 production [17]. Since most of the reports studied the catalytic performance of Cu_2O using metallic Cu as substrates, the catalytic effect of Cu and Cu_2O-Cu interface cannot be excluded. As a result, there is an ongoing debate whether the oxide layer contributes to catalysis, or whether it only acts as a promoter of the well-structured metal catalysts.

Ionic liquids (ILs) have aroused great interest in the past decades due to their unique properties, such as negligible vapor pressure, wide potential window and high conductivity. Recently, Luo *et al.* [18] reported that the natural graphite was electrochemical exfoliated in ionic liquid/water solution to prepare ionic-liquid-functionalized graphene sheets, which can be further gratified to obtain nanocomposites with high structural homogeneity and excellent electrical conductivity.

Herein, we propose a facial strategy to prepare graphite sheets by electro-exfoliation of pure graphite rod assisted by an ionic liquid, with further supporting the Cu_2O nanoparticles (Cu_2O NPs) on the graphite sheets. Because the graphite sheets as prepared are nearly inert for CO_2 electrocatalytic reduction theoretically, it offers a new strategy to study the catalytic performance of Cu_2O independently for CO_2 electroreduction.

2 Experimental

2.1 Materials

1-Octyl-3-methylimidazolium chloride (OmimCl, purity > 99.0%) was purchased from the Centre of Green Chemistry and Catalysis, LICP, CAS, P. R. China. Copper chloride dihydrate (purity ≥ 99.0%), trisodium citrate dehydrate (purity ≥ 99.0%), sodium borohydride (purity ≥ 98.0%), potassium hydrogen carbonate (purity ≥ 99.5%), and ethanol anhydrous (purity ≥ 99.7%) were provided by Sinopharm Chemical Reagent Co., Ltd., P. R. China. Nafion N-117 membranes (0.180 mm thick, ≥ 0.90 $meq \cdot g^{-1}$ exchange capacity) were purchased from Alfa Aesar China Co., Ltd. High purity graphite rod (ø: 3 mm) was purchased from Beijing Crystal Dragon Carbon Technology Co., Ltd., P. R. China. All the reagents were used as received. The water used in all experiments was purified by a Millipore system.

2.2 Preparation of 1-octyl-3-methylimidazole functionalized graphite sheets (ILGS)

The details process of ILGS preparation was described as follows: Two high-purity graphite rods were placed parallel as electrodes in the OmimCl/water (1 : 5, volume ratio) solution with a separation of 2.0 cm. A MS-605D model potentiostat (Shenzhen MST Technology Co., Ltd, P. R. China) was used to provide the potential. Static potentials of 10 V were applied to the two electrodes. After electrolysis for 6 h, a dark red solution appeared. The resulting powder was isolated from the solution by centrifugation, washed with deionized water and ethanol thoroughly, and dried under vacuum at 60 °C for 6 h. Finally, the ILGS was obtained.

As a control experiment, the electrolyte was replaced by 0.1 $mol \cdot L^{-1}$ K_2SO_4 aqueous solution and the un-functionalized graphite sheets (GS) were obtained using the same procedure with ILGS.

2.3 Preparation of Cu_2O/1-octyl-3-methylimidazole functionalized graphite sheets(Cu_2O//ILGS)

The details process of Cu_2O/ILGS preparation were described as follows: 0.0978 g copper chloride dihydrate and 0.0429 g sodium citrate were dissolved in 50 mL deionized water and stirred for 30 min under Ar atmosphere to get a sky-blue solution. 0.06 g ILGS were added to 10 mL deionized water and sonicated for 30 min, an ILGS dispersion solution was obtained. The above two solutions were mixed together and stirred for 30 min under Ar atmosphere. Then, 15 mg sodium borohydride dissolved in water was dropwise added to the mixture under stirring for 20 min vigorously and a dark yellow solution was formed. Finally, the powder product was filtered, following by washed with water and ethanol thoroughly, and dried under vacuum at 60 °C for 12 h. Finally, the Cu_2O/ILGS was obtained.

As a control group, Cu_2O-loaded graphite sheets (Cu_2O/GS) was obtained with the same procedure, except that the ILGS were replaced by GS.

2.4 Materials characterization

The morphology of materials as made was characterized by transmission electron microscopy (TEM, JEM-2010, 220 kV, Japan). X-ray diffraction (XRD, X'Pert PRO MPD, Netherlands) operated at 40 kV and 40 mA (Cu K_α radiation, λ = 0.15406 nm) was used to observe the crystal structure of cuprous oxide and graphite. Raman spectroscopy (Renishaw RM2000, UK) were used to examine the graphitization degree of the obtained samples. The elemental composition and chemical bonding were studied by X-ray photoelectron spectroscopy (XPS, Thermo Scientific Escalab 250XI, USA) with Mg K_α radiation. Typically, the hydrocarbon C 1*s* line at 284.8 eV from adventitious carbon was used for energy referencing.

2.5 CO_2 reduction electrolysis and product analysis

The working electrode was prepared as follows: 1 mg Cu_2O/ILGS was added to 200 μL of ethanol anhydrous. With further adding 5 μL of 5% Nafion solution and sonicated for 20 min to obtain a uniformly dispersed suspension, which was dropped on a L-type glassy carbon electrode (ø: 10 mm) and dried with N_2.

The apparatus and procedures were similar with those reported previously for electrochemical reduction of CO_2 [19–22]. Briefly, the reduction electrolysis was performed under room temperature (25 °C) in an H-type cell with an Ag/AgCl reference electrode (saturated KCl) and a Pt plate (1 cm × 1 cm) counter electrode. 0.1 $mol \cdot L^{-1}$ $KHCO_3$ aqueous solution was used as electrolytes and the cathode and anode compartments were separated by Nafion 117 proton exchange membrane.

Before CO_2 eletrocatalysis, the working electrode (cathode) side was bubbled with Ar for 30 min to discharge the air in the electrolyte. Then CO_2 was bubbled for another 30 min at a flow rate of 20 $mL \cdot min^{-1}$ to saturate the electrolyte.

An electrochemical workstation (CHI 760, Shanghai CH Instruments Co., P. R. China) was used for the potentiostat CO_2 reduction eletrocatalysis experiments. All the measured potentials in this work were cited with respect to the reversible hydrogen electrode (RHE) using the following conversion: E_{RHE} (V) = $E_{Ag/AgCl}$ (V) + 0.197 V + (0.059 V × pH). The pH value of the electrolyte is 6.8 in CO_2 atmosphere. The CO_2 reduction products were detected on a gas chromatograph (North Rayleigh 7890A, P. R. China) with a methanator using flame ionization detector (FID), while the H_2 was tested on the gas chromatography (Shimadzu GC-2014, Japan) using thermal conductivity detector (TCD). The carrier gases of the FID and TCD are nitrogen and argon respectively. The liquid product was tested by UV method [23]. The faradaic efficiency (FE) of all the products was calculated according to the methods established by Yeo *et al.* [15].

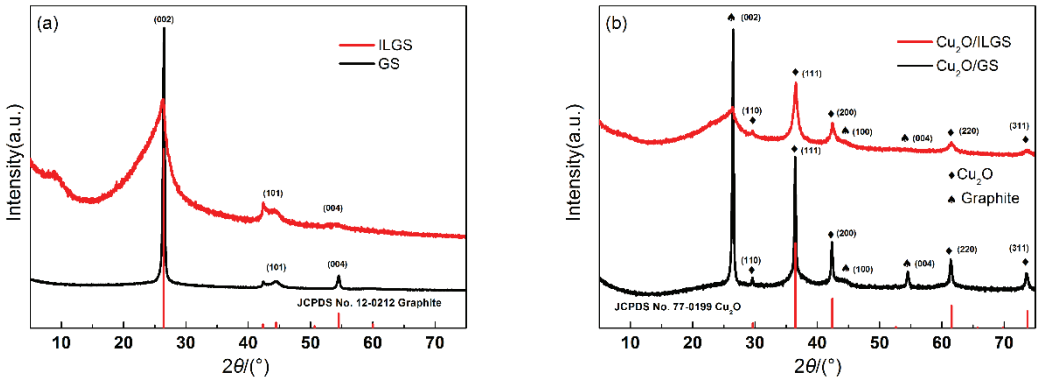

Fig. 1 XRD patterns of (a) ILGS and GS; (b) Cu_2O/ILGS and Cu_2O/GS.

color online.

3 Results and discussion

3.1 Materials characterization

The crystal structure of the materials as made was characterized by XRD, as shown in Fig. 1.

The XRD patterns of GS (Fig.1a, black line) and ILGS (Fig.1a, red line) both exhibit the (002), (101), and (004) graphite diffraction peaks, indicating the structure of graphite is preserved after the electro-exfoliation process [18,24]. However, the (002) peak of ILGS is broader than GS, which hints that ILGS have more defects than GS due to the 1-octyl-3-methylimidazole grafted to the graphite sheets in the electro-exfoliation process [18].

Raman spectroscopy is one of the key analytical techniques used in the characterization of graphite sheets. Fig. 2 shows typical Raman spectra of natural graphite, GS and ILGS. In the Raman spectrum of natural graphite, the G peak at ~1593 cm^{-1} corresponds to an E_{2g} mode of graphite, which is related to the vibration of sp^2-bonded carbon atoms in a 2D hexagonal lattice, such as in a graphite layer. The D peak at ~1353 cm^{-1} is associated with vibrations of carbon atoms with dangling bonds in plane terminations of disordered graphite. The intensity contrast of raw material (Fig. 2, grey line) shows that the intensity of the *G* peak is ten times that of *D* peak (mean I_D/I_G ratio = 0.10), indicating an ideal degree of graphite. The I_D/I_G ratio of GS (Fig. 2, black line) is 0.30, indicating a low degree of defects. On the contrary, the I_D/I_G ratio of ILGS ((Fig. 2, red line)

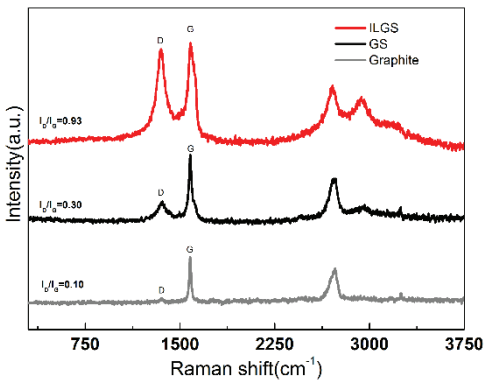

Fig. 2 Raman spectra of ILGS, GS, and graphite raw material.

color online.

is 0.93, indicating a high degree of defects, which is due to the functionalization of graphite sheets by 1-octyl-3-methylimidazole through the electro-exfoliation process.

Except for the characteristic peaks of graphite sheets, the XRD patterns of Cu_2O/GS and Cu_2O/ILGS both exhibit the (110), (111), (200), (220), and (311) diffraction peaks, as labelled in Fig. 1b, which is consistent with polycrystalline Cu_2O (JCPDS 77-0199) [15] and there is no characteristic peak for impurities. The XRD results indicate that pure phase Cu_2O are formed on GS and ILGS.

To further confirm our conclusion, survey XPS spectra of Cu_2O/ILGS were recorded, as displayed in Fig. 3. The total XPS spectrum mainly consists of C, N, O and Cu core-elements, indicating successful deposition of N on ILGS. More specially, the high-resolution C 1*s* spectrum of Cu_2O/ILGS (Fig. 3b) can be deconvoluted to four Gaussian peaks located at 284.76, 285.60, 286.35, 287.35, and 288.70 eV, corresponding to the C＝C, C－C/C－H, C－N, C＝O, and O－C＝O bonds, respectively. Consistently, the high resolution N 1*s* spectrum of Cu_2O/ILGS, as shown in Fig. 3c, can be deconvoluted predominantly into two peaks at 400.42 and 402.15 eV, which corresponds to di-substituted imidazole nitrogen atoms [18]. The result indicates 1-octyl-3-methylimidazole is successfully grafted to the defects of graphite sheets during the electro-exfoliation of graphite rod in the OmimCl/water solution, as shown in Scheme 1.

In addition, the high-resolution Cu 2*p* spectrum (Fig. 3d) for the composite heterostructure shows binding energies of 932.5 and 934.5 eV, corresponding to the Cu $2p_{3/2}$ spin-orbit peaks of Cu^+ and Cu^{2+}, separately. Despite few Cu^+ ions having been oxidized into Cu^{2+}, the XRD patterns indicate that the copper in Cu_2O/ILGS still remain in the pure Cu_2O phase [25].

According to the XPS spectra, the contents of elements in all the materials as made are presented in Table 1. Predictably, the main element in GS and ILGS is carbon, while the oxygen comes from the oxidation of graphite in the electro-exfoliation of graphite rod. There is no N in GS while the N content in ILGS is 3.76%, indicating the N completely comes from the 1-octyl-3-methylimidazole grated to the graphite sheets. Finally, the Cu

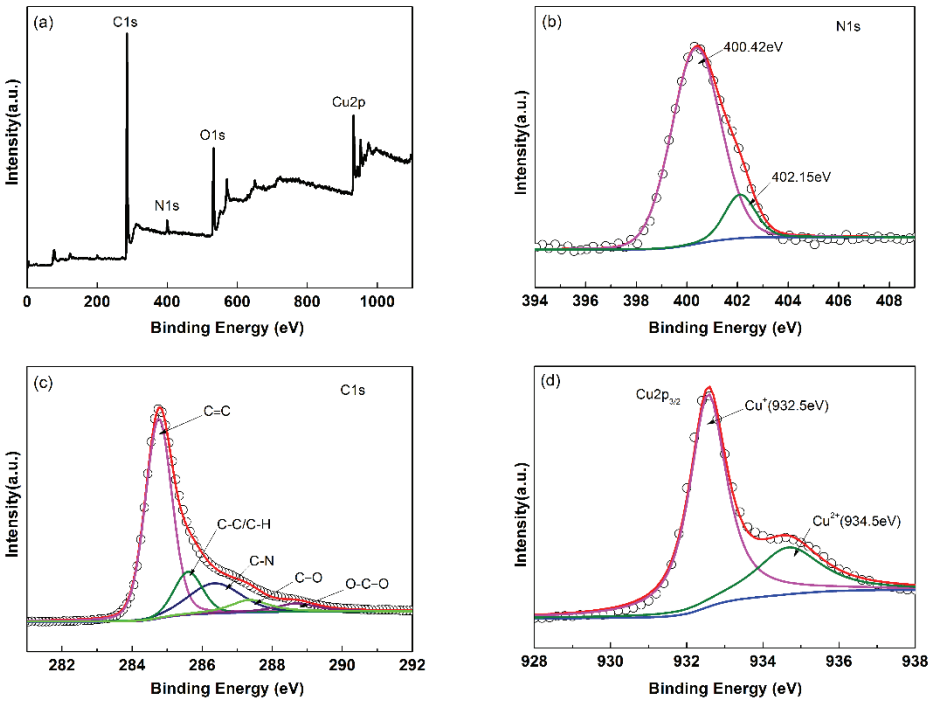

Fig. 3 XPS patterns of Cu_2O/ILGS.

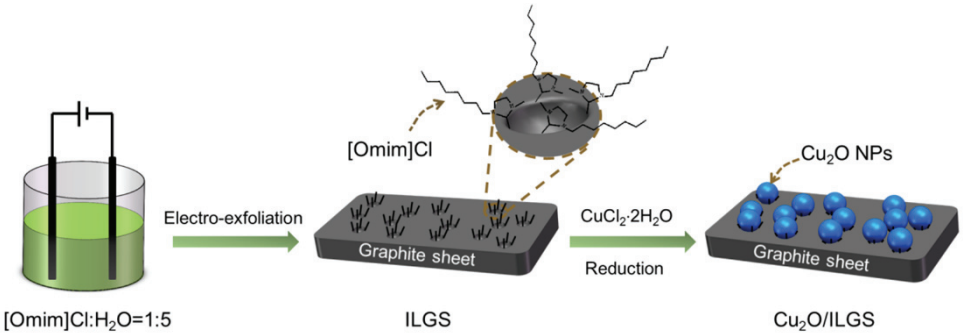

Scheme 1 Synthesis process of Cu_2O/ILGS.

Table 1 Relative contents (atomic fraction, %) of all elements from XPS spectra.

Catalyst	C	O	N	Cu
Cu_2O/ILGS	58.32	25.88	3.34	12.46
ILGS	87.88	8.36	3.76	–
Cu_2O/GS	62.51	25.07	–	12.42
GS	85.5	14.5	–	–

content of Cu_2O/ILGS and Cu_2O/GS is 12.46% and 12.42%, respectively.

The TEM images (Fig. 4a) depict that GS and ILGS are composed of multilayer graphene sheets. The TEM image of Cu_2O/ILGS (Fig. 4c) shows that Cu_2O possess uniform size ranging from 4 to 8 nm with an average diameter of 5 nm (inset of Fig. 4c), while in the Cu_2O/GS (Fig. 4d), the Cu_2O exists obvious aggregation (average diameter of 38 nm), indicating the 1-octyl-3-methylimidazole functionalized graphite sheets can fix the position of Cu_2O by offering anchor positions and inhibit the aggregation of Cu_2O through steric effect, as depicted in Scheme 1.

3.2 CO_2 electrochemical reduction performance

To explore the electrocatalytic performance of Cu_2O/ILGS, the potential electrolysis experiments were carried out at different voltages from −1.0 to −1.4 V (*vs* RHE), the gas in the headspace was collected and analysed by GC, and the liquid mixture was analysed by UV method. It was found that gas product contains CO, CH_4 and C_2H_4, while H_2 is the only by-product. HCOOH is the only product observed in liquid mixtures. The FE of gas products as a function of applied potential using Cu_2O/ILGS as electrode was shown in Fig. 5a. As the voltage increases, the FE of H_2 decreases first and then increases with applied potentials, indicating the hydrogen evolution is a competitive reaction to CO_2 reduction [26]. All the reduction products from CO_2 exists a maximum value when rising the applied potentials, while the FE of ethylene ($FE_{ethylene}$) reached the maximum 14.8% at −1.3 V (*vs* RHE), with 70.9% selectivity in the gas phase products of CO_2 reduction.

To further study the catalytic mechanism of Cu_2O/ILGS, the

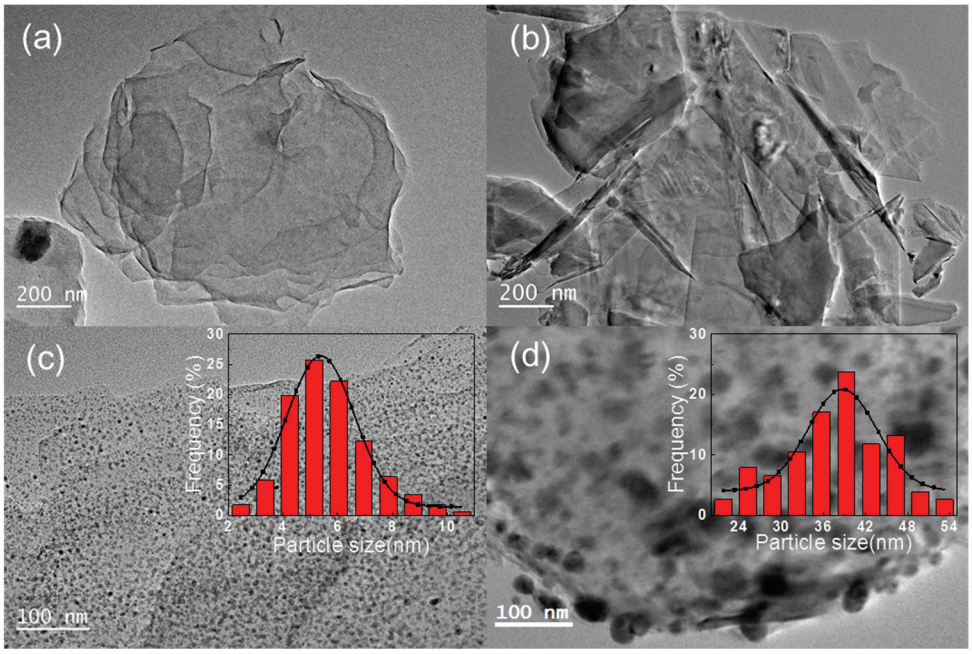

Fig. 4 TEM images for (a) ILGS; (b) GS; (c) Cu_2O/ILGS; (d) Cu_2O/GS.

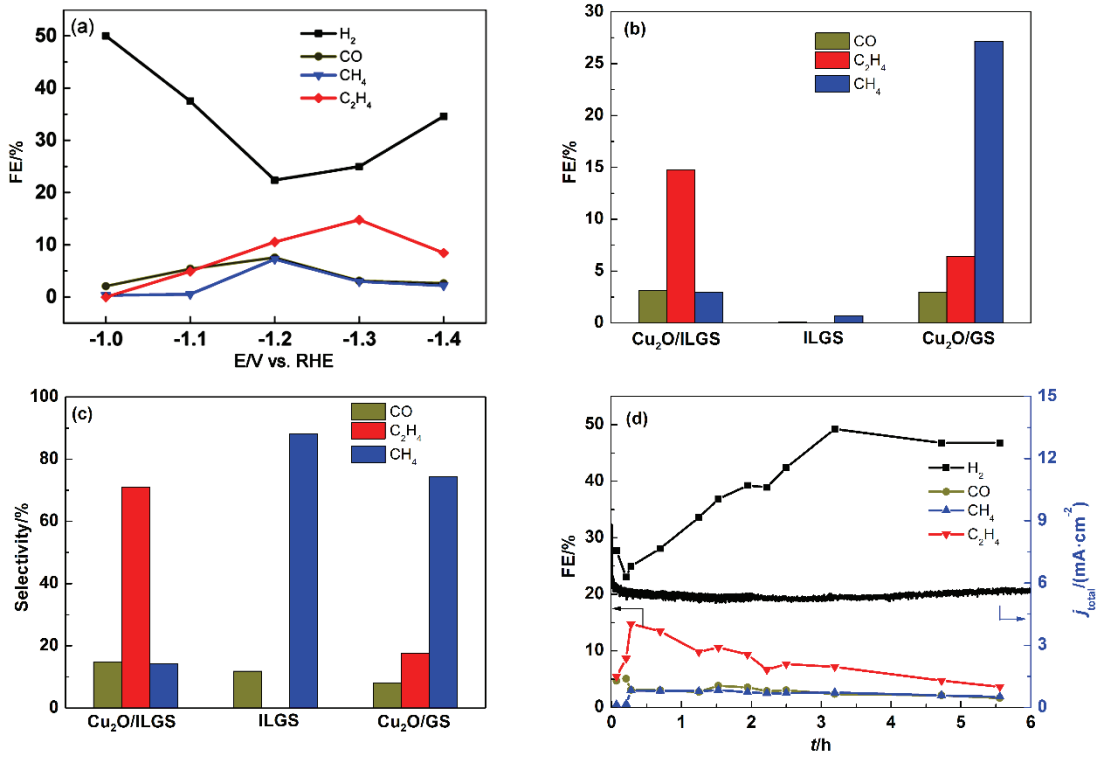

Fig. 5 (a) Fractional faradaic efficiency of gas products; (b, c) Faradaic efficiencies and selectivity of gas products at −1.3 V (*vs* RHE); (d) Faradaic efficiency of gas products and total current density with respect to electrolysis time at -1.3 V (*vs* RHE).

controlled potential electrolysis experiments were carried out at −1.3 V (*vs* RHE) using GS, ILGS and Cu_2O/GS as electrodes, respectively.

When GS was used as catalyst, none of carbon-containing compounds was detected. As for ILGS, only trace amounts of CO and CH_4 were detected but no ethylene. Therefore, Cu_2O is believed to be the main active sites for CO_2 reduction. When using Cu_2O/GS as electrode, the $FE_{ethylene}$ is 6.4%, corresponding to 17.6% selectivity, indicating the activity and selectivity of ethylene are closely related to the size and aggregation of Cu_2O NPs. The 1-octyl-3-methylimidazole grated to graphite may form many special nestle-like structures, which offered anchoring sites for Cu_2O NPs. Meanwhile, the steric effect of 1-octyl-3-methylimidazole prevents the aggregation of Cu_2O NPs during the deposition of Cu_2O. Because of the stabilization effects of ILGS, the Cu_2O NPs are much smaller and more

uniformly dispersed on ILGS, leading to much better catalytic performance than those on GS.

At last, the long-time electrocatalytic performance of Cu_2O/ILGS was studied, as shown in Fig. 5d. During the 6 h electrolysis, the FE of H_2 increased while the FE of CO, CH_4 and C_2H_4 decreased gradually. The decline of $FE_{ethylene}$ may arise from the reduction of Cu_2O to Cu^0 during the electrolysis of CO_2, which was confirmed by XRD pattern (Supporting Information, Fig. S1). The details of structure changes of Cu_2O/ILGS during the CO_2 electroreduction will be further investigated in our future work.

4 Conclusions

In summary, we have successfully developed a facile method to achieve Cu_2O/ILGS composites, which can be used as efficient electrocatalyst for electrochemical reduction of CO_2 to C_2H_4. Under −1.3 V (*vs* RHE), the FE of ethylene is up to 14.8%, which is more than two times of Cu_2O/GS. The high efficient is due to the 1-octyl-3-methylimidazole grafted to graphite sheets by electro-exfoliation method, which can form anchored position for Cu_2O NPs and prevent the aggregation of Cu_2O by steric effect. Our work offers a new strategy to prepare imidazole functionalized graphite sheets as new versatile supports to facilitate the dispersion of metal oxides as catalyst in many other applications.

Supporting Information: available free of charge *via* the internet at http://www.whxb.pku.edu.cn.

References

(1) Song, Y. F.; Chen, W.; Zhao, C. C.; Li, S. G.; Wei, W.; Sun, Y. H. *Angew. Chem. Int. Ed.* **2017,** *56*, 10844. doi: 10.1002/anie.201706777

(2) Chang, X. X.; Wang, T.; Zhang, P.; Wei, Y. J.; Zhao, J. B.; Gong, J. L. *Angew. Chem. Int. Ed.* **2016,** *55*, 8840. doi: 10.1002/anie.201602973

(3) Chang, X. X.; Wang, T.; Gong, J. L. *Energ. Environ. Sci.* **2016,** *9*, 2177. doi: 10.1039/c6ee00383d

(4) Chen, C. S.; Handoko, A. D.; Wan, J. H.; Ma, L.; Ren, D.; Yeo, B. S. *Catal. Sci. Technol.* **2015,** *5*, 161. doi: 10.1039/c4cy00906a

(5) Mistry, H.; Varela, A. S.; Bonifacio, C. S.; Zegkinoglou, I.; Sinev, I.; Choi, Y. W.; Kisslinger, K.; Stach, E. A.; Yang, J. C.; Strasser, P.; *et al. Nat. Commun.* **2016,** *7*, 12123. doi: 10.1038/ncomms12123

(6) Yang, K. D.; Ko, W. R.; Lee, J. H.; Kim, S. J.; Lee, H.; Lee, M. H.; Nam, K. T. *Angew. Chem. Int. Ed.* **2017,** *56*, 796. doi: 10.1002/anie.201610432

(7) Kwon, Y.; Lum, Y.; Clark, E. L.; Ager, J. W.; Bell, A. T. *ChemElectroChem* **2016,** *3*, 1012. doi: 10.1002/celc.201600068

(8) Roberts, F. S.; Kuhl, K. P.; Nilsson, A. *Angew. Chem. Int. Ed.* **2015,** *54*, 5179. doi: 10.1002/anie.201412214

(9) Ye, S. H.; He, X. J.; Ding, L. X.; Pan, Z. W.; Tong, Y. X.; Wu, M. M.; Li, G. R. *Chem. Commun.* **2014,** *50*, 12337. doi: 10.1039/c4cc04108a

(10) Han, Z. J.; Kortlever, R.; Chen, H. Y.; Peters, J. C.; Agapie, T. *ACS Central Sci.* **2017,** *3*, 853. doi: 10.1021/acscentsci.7b00180

(11) Li, Y. F.; Cui, F.; Ross, M. B.; Kim, D.; Sun, Y. C.; Yang, P. D. *Nano Lett.* **2017,** *17*, 1312. doi: 10.1021/acs.nanolett.6b05287

(12) Handoko, A. D.; Chan, K. W.; Yeo, B. S. *ACS Energy Lett.* **2017,** *2*, 2103. doi: 10.1021/acsenergylett.7b00514

(13) Eilert, A.; Roberts, F. S.; Friebel, D.; Nilsson, A. *J. Phys. Chem. Lett.* **2016,** *7*, 1466. doi: 10.1021/acs.jpclett.6b00367

(14) Ma, M.; Djanashvili, K.; Smith, W. A. *Angew. Chem. Int. Ed.* **2016,** *55*, 6680. doi: 10.1002/anie.201601282

(15) Ren, D.; Deng, Y. L.; Handoko, A. D.; Chen, C. S.; Malkhandi, S.; Yeo, B. S. *ACS Catal.* **2015,** *5*, 2814. doi: 10.1021/cs502128q

(16) Lee, S.; Kim, D.; Lee, J. *Angew. Chem. Int. Ed.* **2015,** *127*, 14914. doi: 10.1002/anie.201505730

(17) Kim, D.; Lee, S.; Ocon, J. D.; Jeong, B.; Lee, J. K.; Lee, J. *Phys. Chem. Chem. Phys.* **2015,** *17*, 824. doi: 10.1039/c4cp03172e

(18) Liu, N.; Luo, F.; Wu, H. X.; Liu, Y. H.; Zhang, C.; Chen, J. *Adv. Funct. Mater.* **2008,** *18*, 1518. doi: 10.1002/adfm.200700797

(19) Sun, X. F.; Kang, X. C.; Zhu, Q. G.; Ma, J.; Yang, G. Y.; Liu, Z. M.; Han, B. X. *Chem. Sci.* **2016,** *7*, 2883. doi: 10.1039/c5Sc04158a

(20) Kang, X. C.; Zhu, Q. G.; Sun, X. F.; Hu, J. Y.; Zhang, J. L.; Liu, Z. M.; Han, B. X. *Chem. Sci.* **2016,** *7*, 266. doi: 10.1039/c5sc03291a

(21) Weng, Z.; Zhang, X.; Wu, Y. S.; Huo, S. J.; Jiang, J. B.; Liu, W.; He, G. J.; Liang, Y. Y.; Wang, H. L. *Angew. Chem. Int. Ed.* **2017,** *56*, 13135. doi: 10.1002/anie.201707478

(22) DeCiccio, D.; Ahn, S. T.; Sen, S.; Schunk, F.; Palmore, G. T. R.; Rose-Petruck, C. *Electrochem. Commun.* **2015,** *52*, 13. doi: 10.1016/j.elecom.2015.01.006

(23) Hong, J. D.; Zhang, W.; Ren, J.; Xu, R. *Anal. Methods* **2013,** *5*, 1086. doi: 10.1039/c2ay26270c

(24) Parvez, K.; Wu, Z. S.; Li, R. J.; Liu, X. J.; Graf, R.; Feng, X. L.; Mullen, K. *J. Am. Chem. Soc.* **2014,** *136*, 6083. doi: 10.1021/ja5017156

(25) Zhang, Y.; Wang, X.; Zeng, L.; Song, S.; Liu, D. *Dalton Trans.* **2012,** *41*, 4316. doi: 10.1039/c2dt12461k

(26) Zhu, Q. G.; Sun, X. F.; Kang, X. C.; Ma, J.; Qian, Q. L.; Han, B. X. *Acta Phys. -Chim. Sin.* **2016,** *32*, 261. [朱庆宫, 孙晓甫, 康欣晨, 马珺, 钱庆利, 韩布兴. 物理化学学报, **2016,** *32*, 261.] doi: 10.3866/PKU.WHXB201512101